Photochemical & Photobiological Sciences

PAPER

Cite this: *Photochem. Photobiol. Sci.*, 2016, **15**, 297

Rhodopsins carrying modified chromophores – the 'making of', structural modelling and their light-induced reactivity†

Andreas Ockenfels,[a] Igor Schapiro*[b] and Wolfgang Gärtner*[a]

A series of vitamin-A aldehydes (retinals) with modified alkyl group substituents (9-demethyl-, 9-ethyl-, 9-isopropyl-, 10-methyl, 10-methyl-13-demethyl-, and 13-demethyl retinal) was synthesized and their 11-*cis* isomers were used as chromophores to reconstitute the visual pigment rhodopsin. Structural changes were selectively introduced around the photoisomerizing $C_{11}{=}C_{12}$ bond. The effect of these structural changes on rhodopsin formation and bleaching was determined. Global fit of assembly kinetics yielded lifetimes and spectral features of the assembly intermediates. Rhodopsin formation proceeds stepwise with prolonged lifetimes especially for 9-demethyl retinal (longest lifetime τ_3 = 7500 s, *cf.*, 3500 s for retinal), and for 10-methyl retinal (τ_3 = 7850 s). These slowed-down processes are interpreted as either a loss of fixation (9dm) or an increased steric hindrance (10me) during the conformational adjustment within the protein. Combined quantum mechanics and molecular mechanics (QM/MM) simulations provided structural insight into the retinal analogues-assembled, full-length rhodopsins. Extinction coefficients, quantum yields and kinetics of the bleaching process (μs-to-ms time range) were determined. Global fit analysis yielded lifetimes and spectral features of bleaching intermediates, revealing remarkably altered kinetics: whereas the slowest process of wild-type rhodopsin and of bleached and 11-*cis* retinal assembled rhodopsin takes place with lifetimes of 7 and 3.8 s, respectively, this process for 10-methyl-13-demethyl retinal was nearly 10 h (34670 s), coming to completion only after *ca.* 50 h. The structural changes in retinal derivatives clearly identify the precise interactions between chromophore and protein during the light-induced changes that yield the outstanding efficiency of rhodopsin.

Received 26th August 2015,
Accepted 18th January 2016

DOI: 10.1039/c5pp00322a

www.rsc.org/pps

Introduction

The function of biological photoreceptors is fine-tuned by a precise interplay between chromophore and protein. This has been demonstrated best for the vertebrate visual pigment rhodopsin, where the wild-type protein, many mutated derivatives and also rhodopsins carrying structurally[1,2] and electronically modified chromophores have been investigated with greatest precision.[3–5] Rhodopsin as a paradigm for GPCRs (G-protein coupled receptors)[6] is considered one of the best characterized seven-helix transmembrane proteins.

Visual pigments gain their function through the photochemical activity of their 11-*cis* retinal chromophore (vitamin-A aldehyde), covalently bound to the protein *via* a protonated Schiff base through a lysine residue located in their seventh α-helix. Probably the most impressive proof for this optimized functionality in rhodopsin was found when the native retinal was exchanged for 9-demethyl retinal. This chromophore derivative significantly reduces the capability of the modified rhodopsin to activate the G-protein transducin,[7,8] whereas an introduction of the methyl group from the protein side by mutating glycine 121 for alanine (G121A) rescued the 9-dm retinal-impaired G-protein activation.[8]

The exchange of the genuine retinal chromophore for chemically synthesized retinal derivatives with modified structure or altered electronic properties offers an alternative (sometimes being more precise and less disturbing) to site-directed mutagenesis for the study of chromophore–protein interactions and for the dynamics of photochemical conversions.

Structurally modified retinal derivatives have already allowed deep insight into the precise interactions between chromophore and protein.[7,9–17] The insertion of electronically modified substituents, *e.g.*, 9-halogeno-,[18] 10-fluoro- or 10-chlororetinal,[19] or 12-fluororetinal,[14] but especially the use of

[a]*Max-Planck-Institut für Chemische Energiekonversion, Stiftstrasse 34-36, D-45470 Mülheim, Germany. E-mail: wolfgang.gaertner@cec.mpg.de*
[b]*Fritz Haber Center for Molecular Dynamics, Institute of Chemistry, The Hebrew University of Jerusalem, Jerusalem 91904, Israel. E-mail: igor.schapiro@mail.huji.ac.il*

†Electronic supplementary information (ESI) available. See DOI: 10.1039/c5pp00322a

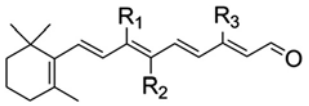

Fig. 1 Structural formula of retinal derivatives used for rhodopsin assembly (depicted in their all-*trans* isomeric state). R_1 = H, C_2H_5, i-C_3H_7, R_2 = H, R_3 = CH_3: 9-demethyl (9dm), 9-ethyl (9et), 9-isopropyl (9-ipr) retinal R_1 = CH_3, R_2 = H, R_3 = CH_3: retinal R_1 = H, C_2H_5, i-C_3H_7, R_2 = H, R_3 = CH_3: 9-demethyl (9dm), 9-ethyl (9et), 9-isopropyl (9ipr) retinal R_1 = CH_3, R_2 = CH_3, R_3 = CH_3, H: 10-methyl- (10me), 10-methyl-13-demethyl (MD) retinal R_1 = CH_3, R_2 = R_3 = H: 13-demethyl (13dm) retinal.

chromophores with structural changes in the vicinity of the photo-isomerizing C_{11}–C_{12} double bond has identified stunning mechanisms in the light-driven reactivity of rhodopsin.[7,11,16,20–22] Here, we demonstrate the effect of structurally changed retinals on rhodopsin formation and the effect of structural changes on the bleaching process. Besides a more detailed analysis of above mentioned 9-demethyl retinal (9dm), effects of 9-ethyl retinal (9et), 9-isopropyl retinal (9ipr), 10-methyl retinal (10me), 13-demethyl retinal (13dm), and 10-methyl-13-demethyl retinal (MD, Fig. 1) on the function of the new pigments formed are reported. Although some effects of these retinal analogues have been reported (cited above), neither the assembly kinetics nor the laser-induced, time-resolved absorption changes upon photo-excitation (bleaching kinetics) have been studied in a quantitative manner. In all cases, samples reconstituted with these retinal derivatives were compared to both native rhodopsin (rh_{nat}) and rhodopsin bleached and *in vitro* assembled with 11-*cis* retinal ($rh_{reconst}$), in order to consider changes in the protein properties upon bleaching and re-assembly.

The experimental results are complemented by hybrid QM/MM simulations of all the synthesized retinal analogues in their rhodopsin-assembled conformation. The calculations allow us drawing conclusions at the molecular level resolution, as crystal structures of the analogue-assembled proteins are not available. Hence, we have structurally optimized the modified retinals within the protein binding pocket and have extended the calculations to all protein sidechains within 4 Å distance to the chromophore.

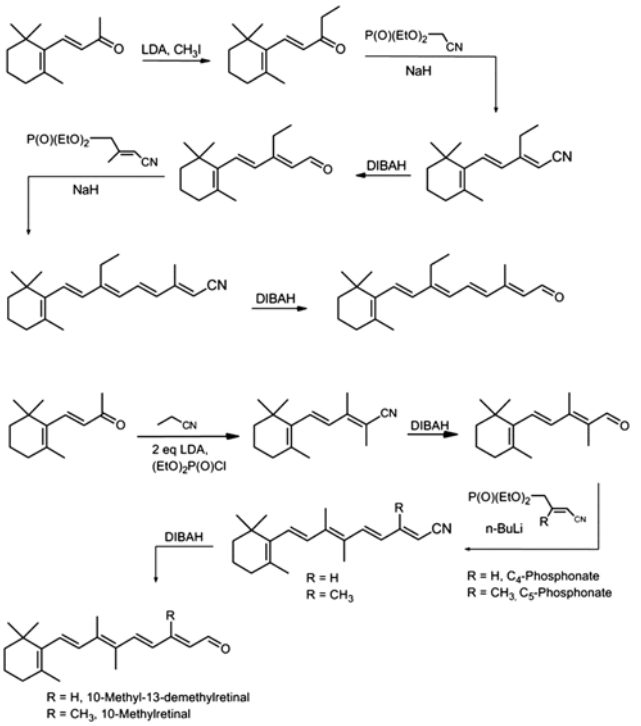

Scheme 1 Reaction strategy for the generation of retinal derivatives carrying structural changes at positions 9 and/or 10 and position 13, exemplified for 9et-, 10me-, and MD (10-methyl-13-demethyl) retinal.

Experimental

Synthetic procedures

Chemical synthesis of retinal derivatives. The chemical synthesis of retinal derivatives employed in this study is briefly outlined in the Results section (see also Scheme 1). Full details and spectral characterization of the synthetic part is given in the ESI.†

Rhodopsin and opsin preparation. Bovine rhodopsin was prepared following standard procedures under safe light (λ > 650 nm).[23] Isolated rod outer segments were placed into hypotonic buffer in order to release other proteins and components yielding the so-called washed membranes. The samples were either kept on ice for direct use or frozen at −40 °C. Rhodopsin concentration was determined by dissolving the washed membranes (50 μL) in a solution of LDAO (3% final concentration, pH 7.2), 10 mM NH_2OH, and 840 μL of Ringer's solution and full bleaching with λ > 470 nm, until no further absorbance change at 500 nm was observed. Routine preparations yielded *ca.* 20 mg mL^{-1} of resuspended washed membranes. All following experiments were performed at pH 7.0–7.2 and at temperature controlled conditions (generally at 20 °C, if not otherwise stated in the text).

Assembly experiments. Formation of novel rhodopsins was performed with a fully bleached rhodopsin, dissolved in Ringer's solution, from which all-*trans* retinal was converted into its oxime and removed by multiple washing steps. A control sample of unassembled opsin was kept in the dark during the assembly experiments and controlled for unwanted reformation of 11-*cis* retinal from residual retinal which would be able to regenerate rhodopsin. No such side reaction was observed over the course of the assembly experiments. Assembly was performed with *ca.* 5 μM opsin solutions, to which a *ca.* 3-fold molar excess of the 11-*cis* isomer of the retinal derivative was added (isopropanol solution, the volume of isopropanol was kept below 3% of the total assembly solution). Injection and mixing of the sample was shorter than 10 s, allowing a most immediate recording of absorbance changes due to chromophore incorporation. At various time points of

the assembly reaction, absorbance spectra were recorded. Assembly of rhodopsins from the retinal derivatives was always accompanied by performing an assembly reaction using 11-*cis* retinal. If not otherwise indicated, all assembly experiments were performed at 20 °C.

Bleaching experiments: determination of extinction coefficients and of bleaching quantum yield. Quantitative bleaching was performed similarly as the rhodopsin content determination, except of using a 487 (±7) nm interference filter and following stepwise bleaching by recording absorbance spectra. Extinction coefficients of rhodopsins assembled with modified chromophores were determined again *via* bleaching of assembled pigments. For this procedure, the extinction coefficient of the oxime forms was determined afore using the all-*trans* isomer of the respective retinal derivative, the concentration of which was determined by an NMR-comparison experiment such that the solution of the retinal derivative for NMR was furnished with a precise amount of toluene. The ratio of signal integrals between the toluene and retinal derivative allowed precise determination of the concentration and thereby of the extinction coefficients of retinal derivatives and their oximes.

Bleaching quantum yields were determined following the method introduced by Dartnall.[24] Briefly, rhodopsins are bleached successively by short irradiation periods with preferentially monochromatic or narrow bandwidth light in the presence of NH_2OH, thus trapping released retinal. The determined ΔA values are then plotted *vs.* time, and the slope of such plot yields the photosensitivity, *i.e.*, the product of quantum yield and extinction coefficient. Plots of ΔA-values from bleaching experiments (applying stepwise irradiation *vs.* time) yield a straight line, the slope of which indicates the photosensitivity, *i.e.*, the product of extinction coefficient and quantum yield.[24,25] Performing such experiments in parallel under identical conditions with a reference compound with known parameters allows extraction of the quantum yield for the unknown species. Bleaching was thus performed in parallel with an 11-*cis* retinal-reconstituted rhodopsin under identical experimental conditions (assembled and native rhodopsin showed identical bleaching kinetics). As the extinction coefficient is determined separately, the quantum yields for rhodopsin with modified chromophores are obtained straightforward. Special care had to be given to rhodopsins carrying chromophores with extremely long-lived intermediates in the bleaching process (see also Results section). Prior to initiation of the bleaching experiments, rhodopsin derivatives were kept in the presence of NH_2OH in the dark in order to control their thermal stability and to trap potentially present unbound retinal.

Laser-induced, time-resolved absorbance changes (flash photolysis). Samples of rhodopsins carrying modified chromophores were prepared for laser-flash photolysis as described above, except that after completion of assembly the excess of retinal derivative was removed by addition of hydroxylamine and centrifugation, discarding the supernatant and employing the pelleted assembled rhodopsins for further measurements. Turbidity was reduced by dissolving the purified rhodopsins in Ringer's solution, containing 1% of dodecyl-β-D-maltoside (DDM). The ratio was *ca.* 0.5 mL mg^{-1} rhodopsin. These detergent suspensions were then diluted to A_{500} = 0.2–0.25. Flash photolysis measurements were always performed under temperature-controlled conditions.

The experimental flash photolysis set-up has been described elsewhere.[26,27] It consisted of an excimer laser-pumped dye laser (Lambda Physik, Göttingen, λ_{exc} = 308 nm, using Coumarin 307 as dye λ_{em} = 500 nm), set geometrically orthogonal to the detection beam line. Detection of absorbance changes was accomplished for recording intervals shorter than 2 ms with a 150 W flash lamp (XBO150, Osram). Longer detection intervals were recorded using a 100 W cw lamp. In order to compensate for baseline drifts and electronic artifacts, the detection light path was split before the sample cuvette and part of the detection light was passed aside the cuvette enabling baseline correction. Two monochromators (slave and a master) were placed before and after the sample cuvette. The signal was detected by a photomultiplier, fed into oscilloscopes (TDS520A or TDS744A, Tektronix) and into a computer for further data handling.

Kinetic analysis was performed applying a home-made fitting software for a global fit analysis that allowed extraction of lifetimes and of lifetime-associated-difference-spectra (LADS) of intermediates. Further treatment of the LADS yielded the pure spectra of the intermediates.[27]

Computational methods. We have studied retinal PSB analogues in the gas phase and in the protein environment. To study the chromophore in the opsin a hybrid quantum mechanics/molecular mechanics (QM/MM) approach[28–30] was used. The QM-MM boundary was placed at the C_δ–C_ε bond between the protonated retinal Schiff base and lysine 296. The QM subsystem was treated using the density functional B3LYP with the 6-31G* basis set. The remainder of the protein compiled the MM subsystem that was evaluated using the Amber[31] force field. The truncated bond was capped using the link-atom scheme by Morokuma and coworkers.[32] The interaction between the QM and MM subsystem is accounted by the electrostatic embedding scheme. For this purpose the Electro-Static Potential Fitted (ESPF) method was applied.[33] In this method the point charges that represent the MM subsystem are interacting with the electron density of the QM subsystem. For the gas phase calculations, we have used the same retinal PSB with a methyl group in order to compare it with the QM/MM simulation. All calculations were done using the Molcas 8.0[34] and Tinker 6.2.[35]

The starting structure relies on the model based on the crystal structure from Okada *et al.*[36] (PDB code 1U19; for details see ref. 36 and details therein). The geometries of the chromophores were optimized using a QM/MM setup in conjuction with microiterative technique[37] and also in the gas phase. In case of QM/MM optimization, the full relaxation included the retinal chromophore, two interior water molecules and all sidechains which have at least one atom within 4 Å distance of the retinal.

The vertical excitation energies were computed using the complete active space second order perturbation theory (CASPT2). This method was applied to study retinal proteins by several groups.[38–48] Its success is based on the favourable error cancelation for excitation energies.[49,50] We have used the B3LYP-optimized geometries together with the ANO-VDZP basis set, according to a recent study by Walczak and Andruniów.[51] The underlying complete active space self consistent field (CASSCF) calculations included the full π-conjugated system in the active space and equally averaged the two lowest states (SA2). The active space comprises 12 electrons in 12 π-type orbitals. In order to account for the dynamic electron correlation complete active space second perturbation theory to second order (CASPT2) was applied in the single state formalism. We used the default IPEA shift of 0.25 a.u. and a level shift of 0.1–0.2 a.u. to avoid intruder states. In order to reduce the computational cost and the computer hardware demands of the two-electron integrals, we used Cholesky decomposition with the default threshold.

Results and discussion

Chemical synthesis of retinal derivatives and 11-*cis* isomer generation and isolation

All retinal derivatives were synthesized following the classical reaction scheme employing the Wittig–Horner variation of carbonyl olefination (Scheme 1, for details see Experimental section and ESI†). Starting material for all compounds was β-ionone. Synthesis of 9dm was not started from cyclo-citral, but instead also from β-ionone which was demethylated by reaction with sodium hypochlorite, thus avoiding difficult separation of α- and β-cyclocitral.[52,53] The synthon for 9et and 9ipr was obtained by mono- and dimethylation of β-ionone,[54,55] whereas a methyl group at position 10 (10me, MD) was introduced by using 2-(di-ethyl-phosphonato)-propionitrile in the reaction with β-ionone.[56] In all cases double bond chain extension was performed with Arbusov reaction-made phosphonates carrying a nitrile functional group that, after double bond formation, was converted in a one-step reaction into the corresponding aldehyde by treatment with di-isobutyl-aluminium-hydride (DIBAL). Separation into the various *trans*- and *cis*-isomers was accomplished by preparative HPLC (for absorption maxima of purified isomers see ESI, Table S1†).[22,57]

The 11-*cis* isomers required for rhodopsin reconstitution were obtained by white light irradiation followed by quantitative HPLC purification under safe light conditions. The intended effect of increased steric constraints due to the introduction of larger substituents, especially at position 10, becomes evident in the UV-Vis spectra of these two retinal derivatives, 10me and MD (Fig. 2). The 11-*cis* isomers of 9dm and 13dm retinal, and also those of 9et and 9ipr showed absorbance spectra very much akin those of the genuine chromophore, whereas both 10-substituted derivatives exhibited remarkably intense '*cis*'-peaks (Fig. 2).

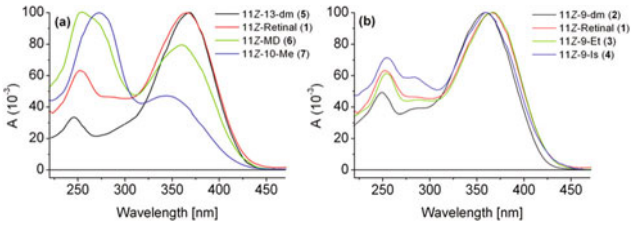

Fig. 2 Absorbance spectra of 11-*cis* isomers of retinal and derivatives, measured in ethanol. 11-*cis* retinal is shown in both panels for comparison.

Structures of the retinal analogues

Based on the QM/MM optimized geometries of the retinal in rhodopsin the modified chromophores can be divided in two subgroups. The first group, comprising 9dm, 13dm and MD, is characterized by small structural changes of the chromophore in relation to the genuine retinal chromophore. They are characterized by the removal or shift of methyl groups to a different position. These modifications leave the retinal backbone geometry (Fig. 3 left) and also the surrounding amino acids nearly unchanged as compared to the wild type structure. One important parameter for the geometry of retinal (and its photochemical activity) is the pre-twist of the C_{11}–C_{12} double bond. For the derivatives in this group, 9dm, 13dm and MD, the C_{10}–C_{11}=C_{12}–C_{13} dihedral angle is −10°, −11° and −23°, respectively. In comparison, the wild type structure shows a twist of −14°. At the first glance it might be surprising that a double bond has a noticeable deviation from planarity. However, the rotational barriers of single bonds are increased in the vicinity of the Schiff base region and comparable to those of double bonds, as shown by Tajkhorshid *et al.*[58] This finding is reflected in a less pronounced bond length alternation pattern close to the Schiff base region, which means the single bonds are contracted and the double bonds are elongated. This was also confirmed in recent work by Walczak and Andruniów.[51] In addition, the *cis* configuration of the C_{11}–C_{12} double bond leads to a slightly stretched bond length as compared to the *trans* counterpart. Moreover, steric interactions with the protein have an impact on the rotation as well.

The second group comprises the derivatives 9et, 9ipr and 10me in which the substitution pattern has a notable impact

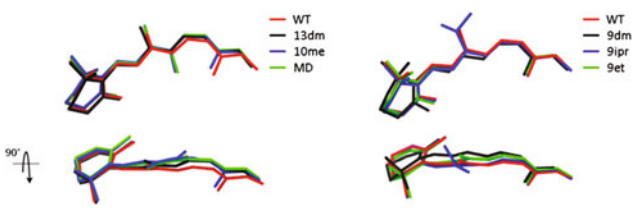

Fig. 3 Retinal geometries. The structures of the retinal analogues derive from QM/MM geometry optimization in rhodopsin; side and top views are provided. For clarity the protein is omitted.

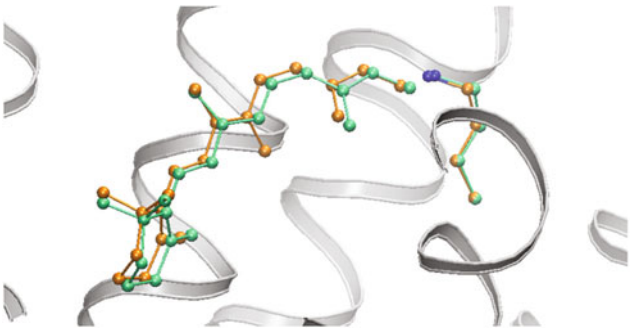

Fig. 4 Comparison of the genuine retinal PSB (green) and the 10me analogue (orange) in the optimized protein binding pocket.

on the structure. Substitution of the methyl group at C_9 by an ethyl or isopropyl moiety increases the steric interaction with the protein. We find that the most stable 9et geometry is characterized by the ethyl group pointing towards tyrosines 191 and 268. Both tyrosine residues are moving slightly away from the retinal chromophore with the conformational change for Tyr191 being larger than that for Tyr268. The isopropyl substituted retinal has increased steric interactions with the methyl group of threonine 118 and the ethyl-sidechain of isoleucine 189, in addition to the interaction with the two tyrosines mentioned above. An additional methyl group at position C_{10} (10me analogue) leads to a strong repulsion with the methyl group at C_{13} (Fig. 3 and 4). Hence, the nature of this interaction is different as compared to the two analogues that are modified at position C_9. This strong repulsion leads to a higher space demand of the 10me retinal analogue. The pretwist of the C_{11}–C_{12} double bond increases to −25° to alleviate the steric interactions, which is almost twice as large as for the wild type. The C_{10}–C_{11}=C_{12}–C_{13} dihedral angle is larger than the single bond twists of C_9=C_{10}–C_{11}=C_{12} (21°) and C_{11}=C_{12}–C_{13}=C_{14} (8°) for the same reasons as explained above. In addition, the whole chromophore is shifted insight the protein binding pocket (Fig. 4).

Absorption maxima and opsin shifts of rhodopsins carrying retinal derivatives

All retinal analogues yielded rhodopsins by incubation with opsin (Table S3†). Two analogues show hypsochromic shifts, *i.e.* 9dm (λ_{max} = 464 nm) and 9ipr (λ_{max} = 490 nm). All other chromophore derivatives yielded absorbance maxima for their assembled pigments in the same spectral range as native rhodopsin or at a slightly larger absorption maximum. A bathochromic shift was observed for both 10-methylated retinals (λ_{max} = 504 nm and 508 nm for MD and for 10me, respectively). The analogues 9et and 13dm show no change in the absorption. 9dm is a particular case, as under all conditions its absorbances are blue-shifted with respect to those of retinal (values in brackets): free aldehyde in ethanol: 374 nm (380 nm), Schiff base with *n*-butylamine: 358 nm (362 nm), protonated Schiff base: 436 nm (444 nm).

Difference (in cm^{-1}) between the absorbance maxima of the rhodopsin (derivatives) and their chromophore protonated Schiff bases (PSB^+) in solution has been termed 'opsin shift' (OS).[59] It identifies the impact of the protein binding site on the electronic properties of rhodopsin's chromophore. OS for native and assembled rhodopsin is determined as 2522 cm^{-1} (for a complete list of all opsin shifts see Table S3†). As the PSB^+ of all retinal derivatives in solution absorb at very similar wavelengths, the strong hypsochromic shift of 9dm-rhodpsin leads to the smallest OS (1384 cm^{-1}). Also 9ipr has a hypsochromic shift (2422 cm^{-1}) compared to retinal, while the opsin shifts caused by all other derivatives are larger than that of the native pigment (9et: 2727 cm^{-1}, 10me: 2636 cm^{-1}, MD: 2580 cm^{-1}, 13dm: 2727 cm^{-1}).

Calculation of excitation energies

The excitation energies were calculated for the optimized QM/MM structures at the CASPT2//B3LYP/ANO-VDZP level of theory. The results are shown along with experimental counterparts in Fig. 5. All values are larger than the experimental values in nm which is in line with the fact that CASPT2 underestimates the excitation energies as compared to more accurate and demanding calculations at higher level of theory.[60] The 9dm retinal analogue shows by far the largest hypsochromic shift, and among all compounds 9dm is the only one lacking a methyl group at position C_9 (removal of a methyl group from position C_{13} apparently has no large effect on the absorption maximum). The flatting of the polyene chain in 9dm retinal geometry alone cannot explain this shift because also 13dm retinal is less distorted. Sugihara and Buss[61] have put forward an electronic effect that explains this shift. Due to the charge transfer that takes place by shifting the electron density from the β-ionone ring towards the Schiff base region there is an additional positive charge on C_7, C_9 and C_{11} atoms. Substitution of the methyl group by a hydrogen at C_9 position

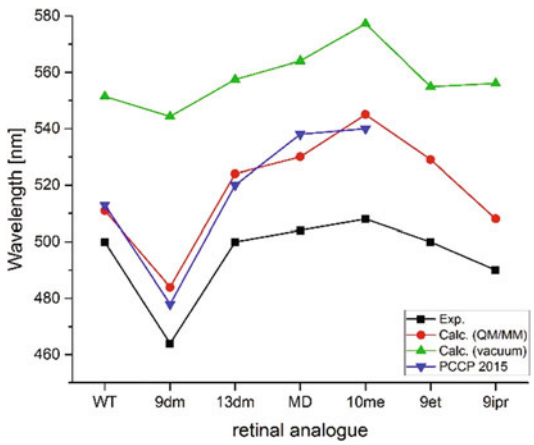

Fig. 5 Excitation energies in nm. Comparison of the experimental and the calculated excitation energies. The calculated values are given for a QM/MM model of rhodopsin (red circles), the retinal PSB analogues in vacuum (green triangles) and the values by Walczak and Andruniów (blue triangles).[51]

destabilizes the positive charge and leads to a destabilization of the excited state. In order to verify this finding we have done additional calculations. The geometry of the protonated retinal Schiff base and the analogues was freely optimized in the gas phase. Hence, the electrostatic and steric interactions with the protein environment were removed. Then we have calculated the excitation energies for these geometries (green line in Fig. 5) and found that also under isolated conditions the 9dm-retinal PSB is the most blue shifted analogue by far. Hence, we conclude the blue shift is a pure electronic effect.

Kinetics of pigment assembly

The rhodopsin assembly process is presented here for three retinal derivatives: 9dm, 9et, and 10me (Fig. 6–8, for further assembly experiments see ESI, Fig. S5 and S6†). Besides the absorbance spectra recorded at different time points during the assembly process, the global fit-derived lifetimes (Table S2†) for the assembly intermediates, their lifetime-associated difference spectra (LADS) and the extracted absolute spectra of the intermediates are shown. Following the convention, LADS with negative amplitudes indicate the formation of an intermediate with the fitted lifetime, whereas positive amplitudes indicate a decaying species, except for the residual absorbance at the end of the process.

The assembly process for 9dm (Fig. 6) is very similar to that of the genuine chromophore 11-*cis* retinal, except of a slight variation of the fitted lifetimes: three lifetimes could be determined of 87, 533, and 7503 s (these numbers are to be considered with tolerance of *ca.* 10%); the corresponding parameters for the genuine retinal chromophore are 101, 387, and 3491 s (see ESI, Fig. S5†). The LADS (Fig. 6c) describe the assembly process: the first identifiable intermediate (τ_1 = 87 s) shows an absorbance maximum around 460 nm, followed by the second intermediate (τ_2 = 533 s), showing a slightly red-shifted maximum around 480 nm. The final process (τ_3 = 7503 s)

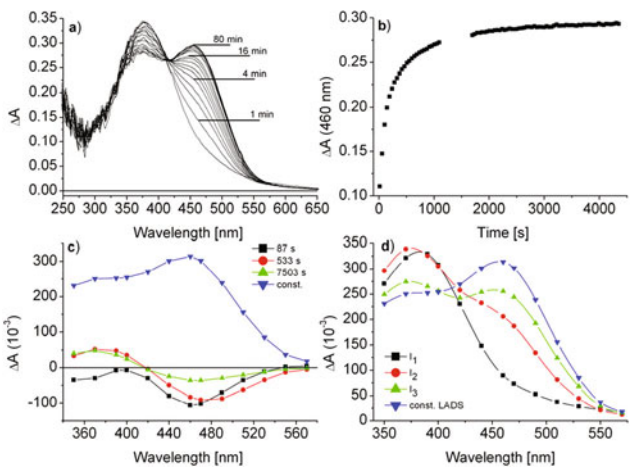

Fig. 6 Rhodopsin assembly process using 9dm retinal as chromophore. (a) Full time course of assembly process; (b) reaction kinetics at absorbance maximum; (c) LADS of assembly from global fit analysis; (d) absolute spectra of assembly intermediates; for details on fitting see text.

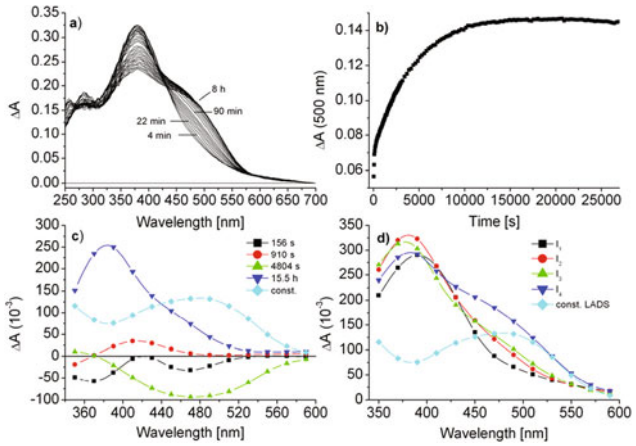

Fig. 7 Rhodopsin assembly process using 9et retinal as chromophore. (a) Full time course of assembly process; (b) reaction kinetics at absorbance maximum; (c) LADS of assembly from global fit analysis; (d) absolute spectra of assembly intermediates; for details on fitting see text.

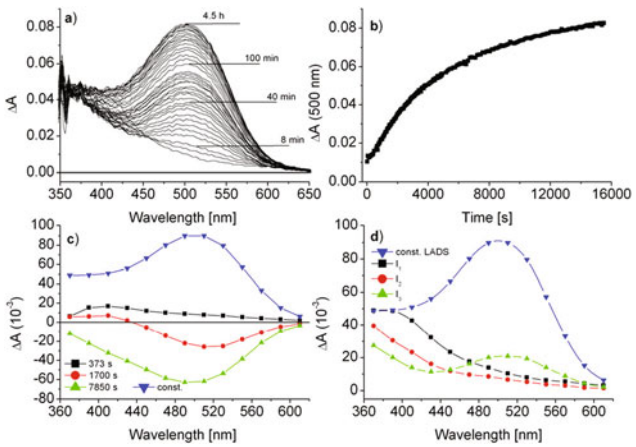

Fig. 8 Rhodopsin assembly process using 10me retinal as chromophore. (a) Full time course of assembly process; (b) reaction kinetics at absorbance maximum; (c) LADS of assembly from global fit analysis; (d) absolute spectra of assembly intermediates; for details on fitting see text.

reflects probably a small conformational change of the protein that causes only a slight variation of the absorbance maximum to the final value of 464 nm.

The extracted absolute spectra of the three intermediates (Fig. 6d) demonstrate the nearly monotonous increase of the absorbance around 460–470 nm and thereby concur with the description obtained from the LADS: the absorbances around 370 nm are due to the free chromophore (which is added as a three-fold molar excess over the protein).

Despite a different overall shape of the assembly spectra, also 9et retinal underwent similar assembly reactions, however, with quite different lifetimes for the various processes of 156, 910, 4804 s, and an additional fourth lifetime of 15.5 h which is outstandingly long-lasting. Whereas the first three lifetimes and also the associated LADS nearly mirror the assembly process of

the native pigment and the above described 9dm assembly reaction, the fourth lifetime of 15.5 h is unexpected. The dominant process for pigment formation (LADS with largest negative amplitude) refers to the lifetime of 4804 s. The longest lifetime (τ_4) of 15.5 h, in contrast, shows a positive amplitude, indicating a decay process and is interpreted as the degradation of the excess chromophore (see also I_4 in Fig. 7c).

Rhodopsin assembly using 10me reveals again a different process with three lifetimes of 373, 1700, and 7850 s (Fig. 8). Only the first of the absolute spectra of the assembly intermediates taken during incubation (lowest absorbance around 500 nm) shows a small peak in the range of the absorbance maximum around 400 nm, all other spectra taken during the assembly reaction only identify a monotonously increasing absorbance around 490 nm. This is in full accordance with the LADS and also with the extracted absolute spectra of the intermediates.

Under routine assembly conditions, 9ipr rhodopsin was only formed by *ca.* 2.5% compared to the yield obtained with 11-*cis* retinal (Fig. S7†), and the reconstituted pigment showed a slightly hypsochromically shifted absorption maximum (λ_{max} = 490 nm). A possible explanation for this observation might be the presence of the bulky isopropyl group at position 9. The low assembly efficiency had also been reported by de Grip *et al.*[23] and, using 9-*n*-propyl retinal, also by Kochendoerfer *et al.*[62] For all other retinal derivatives, the assembly process could even be followed in a time-resolved manner.

As can be expected, 11-*cis* retinal, assembled for comparison, showed the fastest pigment formation kinetics (Table S2†). The more rapid reactions between 80 and 160 s are of similar range as found for the retinal derivatives (except for 10me with τ_1 = 373 s), whereas the final pigment formation (τ_1 *ca.* 3500 s) is shortest of all used retinal compounds.

Quantum yields of rhodopsin bleaching

Quantum yield determination of rhodopsin carrying modified retinals followed the method introduced by Dartnall.[63] In this method stepwise irradiation of rhodopsins is performed in the presence of added hydroxylamine, thus trapping the released chromophore as its oxime. As bleaching for the quantum yield determination is performed in small steps (short irradiation intervals), special care was taken for the accumulation of long-lived bleaching intermediates. Thus, especially for these cases, the dark incubation time was extended to several minutes before the next irradiation was performed.[25] Native rhodopsin (Φ = 0.67) was used as reference. It is common agreement in this type of experiments that the quantum yield refers to the photochemical event, *i.e.*, all following processes are considered taking place with an efficiency of unity without any thermal back reactions to the parental state. All modified rhodopsins bleached with similar quantum yields as the native pigment (between 0.62 for 13dm retinal and 0.71 for 10me retinal), except for the pigment carrying the MD chromophore for which a lower quantum yield of Φ = 0.52 was calculated.

Determination of the quantum yield for this pigment, however, was impeded due to its instability towards hydroxyl amine already in the dark (Fig. S8†). Therefore, bleaching of the MD-containing rhodopsin was performed with a very low hydroxyl amine concentration of only 50 μM, whereas bleaching of all other pigments was performed with a hydroxyl amine concentration of 10 mM (the 9dm-pigment was bleached in presence of 50 mM of hydroxyl amine). It can be assumed that this modified experimental set-up impaired the precision of the quantum yield determination.

Although the bleaching quantum yields for all assembled rhodopsins (with native and derivative chromophores) were very similar, their bleaching kinetics showed remarkable differences. For most pigments a dark incubation period of five minutes was sufficient to bring to completion all absorbance changes induced by the short irradiation intervals. A waiting time of ten minutes was required in case of 13dm rhodopsin to bring all absorbance changes to an end, before the next irradiation period was started. For 9dm rhodopsin, a waiting time of at least 20 minutes was required before the thermal processes came to an end before the next irradiation could be performed. Already these steady-state bleaching experiments gave indications for changed light-induced reaction pathways of rhodopsins carrying structurally modified chromophores calling for a time-resolved observation of the bleaching process.

Laser flash-induced photochemistry

A detailed analysis of the visual pigment bleaching process requires – in contrast to the bleaching quantum yields described above – a very short laser flash as applied in photolysis experiments. Light-induced time-resolved absorbance changes were recorded for all modified rhodopsins, except for the 9ipr-containing pigment, taking native (or bleached/re-assembled) rhodopsin as a reference. With the experimental set-up used, the bleaching process could be followed from *ca.* 0.5 μs up to several hundred ms. For clarity the time-resolved bleaching is also shown here for native rhodopsin (Fig. 9 and Table 1): the formation and decay of the various intermediates are well identified in the flash photolysis experiment. LADS reveal the conversion of bathorhodopsin (part of the LADS with positive amplitude around 570 nm) into the lumi intermediate (negative part of LADS with maximal amplitude around 470 nm) with a lifetime of 0.4 μs. After formation of lumirhodopsin, two other processes with small absorbance changes could be resolved (lifetimes of 124 μs and 815 μs) that can be ascribed to the lumi-to-meta-I transition. As both intermediates absorb in a similar wavelength range, only small absorbance differences should result. The dominant process is then identified in the conversion of meta-I into meta-II rhodopsin with a lifetime of 4.2 ms. This LADS features a positive lobe around 490 nm and a negative lobe (not fully resolved at its high energy flank below 420 nm) indicative for the meta-II intermediate. Further processes (lifetimes of 22 ms and 7 s) cannot exactly be ascribed to individual processes due to the equilibria between the various meta states.[64–66] Rhodopsin obtained by assembly of opsin with 11-*cis* retinal showed the same features as native rhodopsin (data not shown).

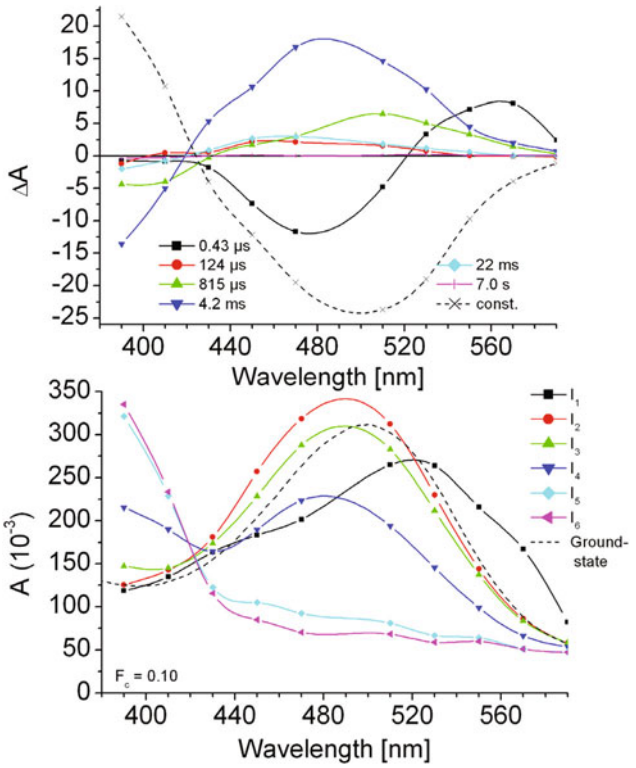

Fig. 9 Laser flash-induced, time resolved absorbance changes in native rhodopsin. (Top) LADS from global fit analysis; (bottom) absolute spectra of bleaching intermediates.

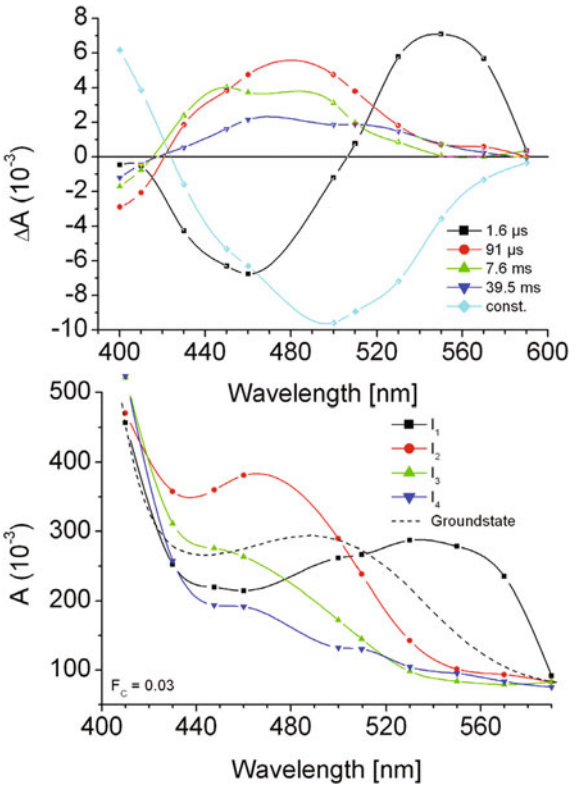

Fig. 10 Laser flash-induced, time resolved absorbance changes in rhodopsin carrying 9et retinal as chromophore. (Top) LADS from global fit analysis; (bottom) absolute spectra of bleaching intermediates.

The photochemistry of 9et-rhodopsin, the most similar to native rhodopsin, already showed different lifetimes (Fig. 10 and Table 1). All other modified rhodopsins displayed entirely different photochemical reactions (see below). Kinetic analysis of 9et-rhodopsin photochemistry revealed lifetimes of τ_{1-4} = 1.6 µs, 91 µs, 7.6 ms, and 39.5 ms, respectively, reflecting the conversion of batho- into lumirhodopsin (τ_1), formation of meta-I rhodopsin (τ_2), and the formation of meta-II rhodopsin in a two-step process ($\tau_{3,4}$). Overall, the lifetimes for these conversions are all slightly longer than those for the corresponding processes in native rhodopsin.

An entirely different photochemical reactivity was determined for 9dm-rhodopsin. During the time interval recordable by the photolysis set-up, practically no photochemical activity was detected (Fig. 11a, note that the 'constant' at the end of the data recording interval has nearly the same spectral shape as the parental state of 9dm-rhodopsin). However, a more precise inspection of the absorbance band present *ca.* 1 s after the laser excitation reveals that this absorbance is red-shifted (λ_{max} = 485 nm) with respect to the parental state of 9dm-rhodopsin (λ_{max} = 464 nm). Transfer of the sample into a spectrophotometer then disclosed the light-induced processes of this pigment: the entire process of bleaching required *ca.* ten hours to come to completion (Fig. 11b). The recorded difference spectra show a monotonous conversion of the lumi-/meta-I state into the unprotonated, blue-shifted meta-II/

Table 1 Lifetimes for bleaching intermediates, obtained from LADS by global fit of flash photolysis experiments; values given in *italics* have been determined by spectrophotometric measurements

	9dm	rh_{nat}	$rh_{reconst}$	9et	13dm	MD	10me
τ_1	0.68 µs	0.43 µs	0.46 µs	1.6 µs	2.0 µs	236 µs	0.33 µs
τ_2	352 ms	124 µs	68 µs	91 µs	184 µs	0.54 s	217 µs
τ_3	*1860 s*	815 µs	886 µs	7.6 ms	76.4 ms	*486 s*	17.6 ms
τ_4	*2340 s*	4.2 ms	4.1 ms	39.5 ms	217 ms	*3223 s*	182 ms
τ_5	*9840 s*	22 ms	23 ms		3.53 s	*5306 s*	573 ms
τ_6		7.0 s	3.8 s		*720 s*	*34 670 s*	*727 s*
τ_7					*2972 s*		*1480 s*
τ_8							*6801 s*

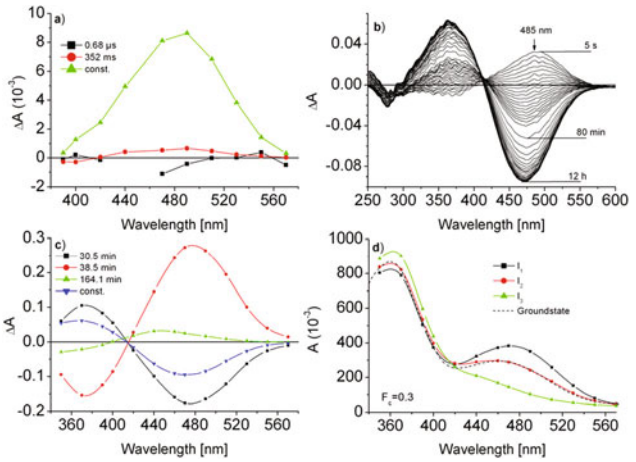

Fig. 11 Laser flash-induced, time resolved absorbance changes in rhodopsin carrying 9dm retinal as chromophore. (a) Observable processes (LADS) by laser flash photolysis instrumentation; (b)–(d) spectrophotometric detection of 9dm rhodopsin bleaching; (b) full time course of bleaching; (c) LADS of bleaching intermediates from global fits analysis; (d) absolute spectra of bleaching intermediates.

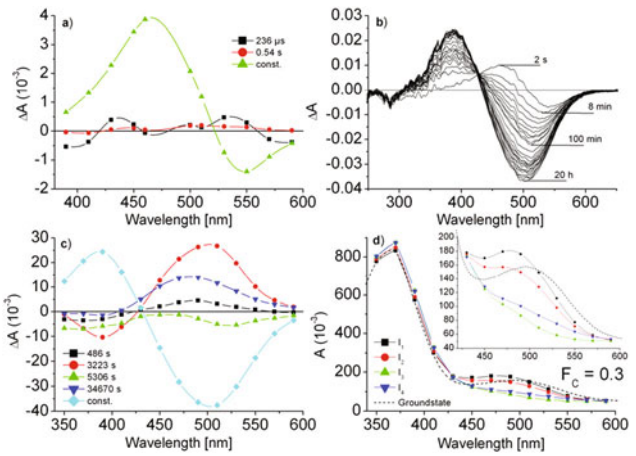

Fig. 12 Laser flash-induced, time resolved absorbance changes in rhodopsin carrying the DM derivative (10-methyl-13-demethyl retinal) as chromophore. (a) Observable processes (LADS) by laser flash photolysis instrumentation; (b)–(d) spectrophotometric detection of DM rhodopsin bleaching; (b) full time course of bleaching; (c) LADS of bleaching intermediates from global fits analysis; (d) absolute spectra of bleaching intermediates.

meta-III forms of 9dm-rhodopsin. These late conversions apparently enclose equilibria between the meta forms, as can be deduced from the LADS and also from the extracted absolute spectra of the intermediates (Fig. 11c and d).

Even more dissimilar are the photochemical processes observed for the MD derivative (10-methyl-13-demethyl retinal, Fig. 12). During the monitoring interval of the laser flash experiment no identifiable processes were observed, however, the remaining 'constant' after several seconds is composed of a partially bleached portion (around 540 nm) and a remaining positive absorbance with maximum around 460 nm (Fig. 12a). As for the derivative described before, also this derivative (MD-rhodopsin) was transferred to a spectrophotometer, due to the assumed long-lived intermediates being formed, and the absorbance changes followed over a longer time period. It turned out that even after *ca.* 20 h (72 000 s) the bleaching process was not complete. The first difference spectrum of the recorded absorbance changes (Fig. 12b, spectrum after 2 s) identifies an initial bleach of the parental state, from which an intermediate with an absorbance maximum around 460 nm is formed. This intermediate species then decays into the meta-II form. The LADS (Fig. 12c) and the derived absolute spectra of the intermediate species (Fig. 12d) identify the underlying processes: analysis of the slow kinetics yields four lifetimes (τ_{1-4} = 486 s, 3223 s, 5306 s, and 34 670 s) which can be ascribed to the conversion of the lumi- and meta-I states and then into the meta-II form. These conversions are accompanied by equilibria as is evident from the LADS found for the lifetime of 5306 s, which exhibits a small absorbance increase around 560 nm (negative lobe of these LADS). Apparently, the strong structural modifications of this retinal derivative cause obstacles in the overall formation process of the meta-II and finally the meta-III state.

Conclusions

The bleaching process of rhodopsin, *i.e.*, the activation of this photoreceptor for interaction with the G-protein transducin has been subject of an enormous number of experiments, including various preparation methods of the pigment.[3] Also the effect of the lipid environment on the thermal stability of rhodopsin has been studied.[67] Additionally, the presence of the all-*trans* isomer of the chromophore (after photoexcitation) and its involvement in the bleaching process during the final steps and its interaction with transducin were revealed.[68] All of these effects demonstrate the outstandingly sophisticated interaction of the chromophore and protein, which enable the functioning of this remarkable molecular machine. Studies employing structurally modified (and stable isotope-enriched) retinals as chromophores[69] have a tradition as long as the modifications of the protein moiety, by equally adding essential information on rhodopsin's function.

Here reported experiments, using retinal derivatives with structural changes around the photoisomerizing C_{11}–C_{12}-double bond as chromophores in rhodopsin, clearly demonstrate the subtle interplay between chromophore and protein. As mentioned, some of these derivatives had been studied in great detail, thus, in the present work we have added insight from QM/MM-based structural calculations and the laser-flash induced time resolved measurements of the bleaching process. Whereas the immediate process of photoisomerization might be impeded to some extent,[70] though not causing fatal effects for the overall bleaching process, it is more the formation and the thermal stability of the late intermediates that

are significantly hindered, indicative by the remarkably extended lifetimes of intermediates found for some of the retinal derivatives. Effects of structural changes had been reported also for 9-, 10-, and 12-halogeno retinals,[14,18,19] yet, an interpretation of these experiments had to discriminate between a steric and an electronic effect due to the introduction of a halogen atom at positions 9, 10, or 12. In the experiments reported here the observed effects are purely due to increased steric interactions between the chromophore and the protein in these novel rhodopsins. Consequences of the modified substitution pattern are eminent in the light-induced reactions that eventually cause bleaching but are also seen for the assembly process. Retinals with increased steric demand had been used in protein–chromophore interaction studies,[10,11,16,20,71,72] however, in most studies effects on the bleaching kinetics were reported only in a qualitative manner.

Of paramount evidence is the finding that some retinal derivatives induce remarkable thermal stability of the late intermediates of the bleaching process, such that monitoring of the full bleaching process and the spectral recording of the late intermediates was only possible within a spectrophotometer, as the detection time range of the laser flash set-up was by far too short to follow the complete bleaching process. The most peculiar results were obtained for 9dm-rhodopsin. This rhodopsin analogue had been studied also by other groups[8,52] and their qualitative findings fully concur with our results. Here we could add quantitative measures employing the global fit analysis, even for processes so slow that they were followed by steady state spectroscopy. Still, it was possible to extract the lifetimes and also the spectral features of the late intermediates that now give a full view on the light-induced interactions between the opsin and the chromophore. The 9dm derivative stands out from all the retinal analogues studied here with respect to the blue absorbance maximum for the rhodopsin-bound form and for the bleaching process which has significant effect on G-protein activation. Still detailed information is elusive how this demethylation effects the processes at the surface of rhodopsin where the binding site for the G-protein is formed.

Assembly process

Rhodopsin formation could be accomplished for all structurally modified retinals, although limits are seen for 9ipr retinal, which could only be assembled by 2–3%. As extended incubation times did not increase pigment formation, one may assume that an equilibrium between bound and unbound 9ipr retinal has been established as a consequence of the bulky isopropyl substituent at position 9. This phenomenon had already been observed by de Grip *et al.*[20] who already suggested (now proven by the here identified assembly intermediates) that the assembly process apparently is a more complex process with intermediate conformational arrangements for the chromophore. The most rapid pigment formation found for the genuine chromophore could have been expected, however, the prolonged assembly reactions determined for several of the retinal derivatives yields interesting insights into the processes of pigment formation. Removal of 'anchor points' (9dm and 13dm retinals) causes a slowing-down of the assembly process by more than a factor of 2 especially for 9dm retinal (τ_3 = 7500 s compared to 3500 s for 11-*cis* retinal; a lesser effect is found for the corresponding 13-demethyl compound, τ_3 = 5234 s), pinpointing the eminent role of the methyl group at position 9 for establishing a functional rhodopsin. This finding meets nicely the formerly reported diminished transducin activation from a 9dm-containing rhodopsin and the signaling recovery by a 'double mutation' 9dm retinal + G121A.[73,74] The importance of this part of the chromophore around position 9 for correct incorporation of the chromophore is also seen by the effect arising from an increase in spatial demand, as accomplished by 10me retinal. This compound showed an even further reduced assembly rate (τ_3 = 7850 s, Fig. 8). Interestingly, an ethyl group at position 9 (9et) slightly slows-down the assembly process (τ_3 = 4800 s, Fig. 7), but does not cause serious obstacles in pigment formation.

Quantum yields

A number of studies had determined quantum yields for retinal derivatives with values partially deviating from the ones determined here. This is particularly the case for 13dm-[62,70,75] and for the MD-assembled rhodopsin.[22,62]

Quantitative bleaching of 13dm rhodopsin revealed a side reaction

Whereas other rhodopsins studied here showed a clear two-state conversion as documented from the isosbestic point and the difference spectra, a shift of baseline and isosbestic point was observed for 13dm rhodopsin (Fig. S8,† last panel). Such behaviour is indicative for formation of an intermediate during the bleaching experiment (see also ref. 25). Such intermediate would cause a filter effect and interfere with the quantum yield determination. Furthermore, both retinal derivatives for which significantly deviating quantum yields (and bleaching behaviour) were reported, showed a strong stability dependence from the added detergents. 13dm- and MD-rhodopsin are fairly stable in the dark when kept in DDM, whereas addition of *N*,*N*-dimethyldodecylamin-*N*-oxide (LDAO) in both cases led to compete loss of the chromophore after 90 to 120 min (Fig. S8 and S9†). This effect might at least in part explain the various deviating values reported in the literature.

Lifetimes of bleaching intermediates as an effect of structurally modified retinals

Surely the most surprising results from this study are the unexpectedly long lifetimes of bleaching intermediates found for some of the structurally modified retinals. It gives the impression that after the photochemical event (that might be hampered to small extent) especially the later-on following conformational changes, *i.e.*, the rearrangement of the proteins around the isomerization-generated new chromophore structure, are 'confronted' with geometric obstacles, either

experiencing too large steric interactions or otherwise experiencing chromophores (especially the demethylated one) that show too much conformational freedom within the binding site.

The bleaching process of rhodopsin, following its ultrafast isomerization is clearly more complex than a mere 'rearrangement' of the protein cavity indicative by the conversion of the red-shifted batho intermediate into the nearly parental state-like absorption of lumirhodopsin. The mechanisms and chromophore–protein interactions for each process, assembly and bleaching must be considered following different reaction pathways. Retardation or only partial assembly is found for sterically demanding, but also for dm retinals. Although these chromophore derivatives also yield differences in the rapid bleaching cascade (as seen, *e.g.*, as a retarded meta-II decay), we are reluctant to propose similar chemical interactions to the protein for both processes, assembly and bleaching, best documented by the assembly process of retinals modified at position 9: 9dm is slow in assembly, 9et behaves nearly as the natural chromophore, whereas 9ipr practically does not assemble. Apparently, both partners chromophore and protein require conformational freedom to follow the reaction pathway, but they mutually control each other's conformational motions like interacting gearwheels to establish and to maintain the meta-II signaling state.

Acknowledgements

We thank the Max-Planck-Society for continuous financial support. A. O. was a recipient of a Ph.D. grant from the Friedrich-Ebert-Foundation.

References

1 I. Szundi, A. R. de Lera, Y. Pazos, R. Alvarez, M. Oliana, M. Sheves, J. W. Lewis and D. S. Kliger, *Biochemistry*, 2002, **41**, 2028–2035.
2 U. M. Ganter, W. Gärtner and F. Siebert, *Eur. Biophys. J.*, 1990, **18**, 295–299.
3 K. Palczewski, *Vertebrate Phototransduction and the Visual Cycle, Part A*, Elsevier BV, San Diego, CA, 2000.
4 O. P. Ernst, D. T. Lodowski, M. Elstner, P. Hegemann, L. S. Brown and H. Kandori, *Chem. Rev.*, 2014, **114**, 126–163.
5 K. Palczewski, *Vertebrate Phototransduction and the Visual Cycle, Part B*, Elsevier BV, San Diego, CA, 2000.
6 K. P. Hofmann, P. Scheerer, P. W. Hildebrand, H.-W. Choe, J. H. Park, M. Heck and O. P. Ernst, *Trends Biochem. Sci.*, 2009, **34**, 540–552.
7 C. K. Meyer, M. Böhme, A. Ockenfels, W. Gärtner, K. P. Hofmann and O. P. Ernst, *J. Biol. Chem.*, 2000, **275**, 19713–19718.
8 M. Han, M. Groesbeek, S. O. Smith and T. P. Sakmar, *Biochemistry*, 1998, **37**, 538–545.
9 K. Nakanishi, N. Berova, N. Fishkin and N. Fujioka, *J. Chin. Chem. Soc.*, 2002, **49**, 443–451.
10 F. DeLange, P. H. M. Bovee-Geurts, J. VanOostrum, M. D. Portier, P. J. E. Verdegem, J. Lugtenburg and W. J. DeGrip, *Biochemistry*, 1998, **37**, 1411–1420.
11 M. A. Verhoeven, P. H. M. Bovee-Geurts, H. J. M. de Groot, J. Lugtenburg and W. J. DeGrip, *J. Mol. Biol.*, 2006, **363**, 98–113.
12 L. U. Colmenares and R. S. H. Liu, *Tetrahedron*, 1996, **52**, 109–118.
13 J. Ni, J. Liu, L. U. Colmenares and R. S. H. Liu, *Tetrahedron Lett.*, 2001, **42**, 1643–1644.
14 P. H. M. Bovee-Geurts, I. Fernández Fernández, R. S. H. Liu, R. A. Mathies, J. Lugtenburg and W. J. DeGrip, *J. Am. Chem. Soc.*, 2009, **131**, 17933–17942.
15 J. W. Lewis, G.-B. Fan, M. Sheves, I. Szundi and D. S. Kliger, *J. Am. Chem. Soc.*, 2001, **123**, 10024–10029.
16 R. Vogel, G. B. Fan, S. Ludeke, F. Siebert and M. Sheves, *J. Biol. Chem.*, 2002, **277**, 40222–40228.
17 G. Fan, F. Siebert, M. Sheves and R. Vogel, *J. Biol. Chem.*, 2002, **277**, 40229–40234.
18 Y. Wang, P. H. M. Bovee-Geurts, J. Lugtenburg and W. J. DeGrip, *Biochemistry*, 2004, **43**, 14802–14810.
19 R. S. H. Liu, F. Crescitelli, M. Denny, H. Matsumoto and A. E. Asato, *Biochemistry*, 1986, **25**, 7026–7030.
20 W. J. de Grip, P. H. M. Bovee-Geurts, Y. Wang, M. A. Verhoeven and J. Lugtenburg, *J. Nat. Prod.*, 2011, **74**, 383–390.
21 R. Vogel, S. Lüdeke, F. Siebert, T. P. Sakmar, A. Hirshfeld and M. Sheves, *Biochemistry*, 2006, **45**, 1640–1652.
22 D. Koch and W. Gärtner, *Photochem. Photobiol.*, 1997, **65**, 181–186.
23 W. J. de Grip, F. J. M. Daemen and S. L. Bonting, in *Methods in Enzymology, Vitamins and Coenzymes Part F*, ed. D. B. McCormick and L. D. Wright, Academic Press, 1980, vol. 67, pp. 301–320.
24 H. J. A. Dartnall, C. F. Goodeve and R. J. Lythgoe, *Proc. R. Soc. London, A*, 1936, **156**, 158–170.
25 W. Gärtner, D. Ullrich and K. Vogt, *Photochem. Photobiol.*, 1991, **54**, 1047–1055.
26 J. M. Strassburger, W. Gärtner and S. E. Braslavsky, *Biophys. J.*, 1997, **72**, 2294–2303.
27 P. Schmidt, T. Gensch, A. Remberg, W. Gärtner, S. E. Braslavsky and K. Schaffner, *Photochem. Photobiol.*, 1998, **68**, 754.
28 A. Warshel and M. Levitt, *J. Mol. Biol.*, 1976, **103**, 227–249.
29 H. M. Senn and W. Thiel, *Angew. Chem., Int. Ed.*, 2009, **48**, 1198–1229.
30 A. Warshel, *Angew. Chem., Int. Ed.*, 2014, **53**, 10020–10031.
31 V. Hornak, R. Abel, A. Okur, B. Strockbine, A. Roitberg and C. Simmerling, *Proteins: Struct., Funct., Bioinf.*, 2006, **65**, 712–725.
32 T. Vreven, K. Morokuma, Ö. Farkas, H. B. Schlegel and M. J. Frisch, *J. Comput. Chem.*, 2003, **24**, 760–769.
33 N. Ferré and J. G. Ángyán, *Chem. Phys. Lett.*, 2002, **356**, 331–339.

34 F. Aquilante, J. Autschbach, R. K. Carlson, L. F. Chibotaru, M. G. Delcey, L. De Vico, I. F. Galván, N. Ferré, L. M. Frutos, L. Gagliardi, M. Garavelli, A. Giussani, C. E. Hoyer, G. Li Manni, H. Lischka, D. Ma, P. Å. Malmqvist, T. Müller, A. Nenov, M. Olivucci, T. B. Pedersen, D. Peng, F. Plasser, B. Pritchard, M. Reiher, I. Rivalta, I. Schapiro, J. Segarra-Martí, M. Stenrup, D. G. Truhlar, L. Ungur, A. Valentini, S. Vancoillie, V. Veryazov, V. P. Vysotskiy, O. Weingart, F. Zapata and R. Lindh, *J. Comput. Chem.*, 2015, DOI: 10.1002/jcc.24221.

35 J. W. Ponder and F. M. Richards, *J. Comput. Chem.*, 1987, **8**, 1016–1024.

36 T. Okada, M. Sugihara, A.-N. Bondar, M. Elstner, P. Entel and V. Buss, *J. Mol. Biol.*, 2004, **342**, 571–583.

37 F. Melaccio, M. Olivucci, R. Lindh and N. Ferré, *Int. J. Quantum Chem.*, 2011, **111**, 3339–3346.

38 A. Strambi, P. B. Coto, L. M. Frutos, N. Ferré and M. Olivucci, *J. Am. Chem. Soc.*, 2008, **130**, 3382–3388.

39 S. Sekharan and V. Buss, *J. Am. Chem. Soc.*, 2008, **130**, 17220–17221.

40 J. S. Frähmcke, M. Wanko, P. Phatak, M. A. Mroginski and M. Elstner, *J. Phys. Chem. B*, 2010, **114**, 11338–11352.

41 G. Tomasello, G. Olaso-González, P. Altoè, M. Stenta, L. Serrano-Andrés, M. Merchán, G. Orlandi, A. Bottoni and M. Garavelli, *J. Am. Chem. Soc.*, 2009, **131**, 5172–5186.

42 T. Andruniów and M. Olivucci, *J. Chem. Theory Comput.*, 2009, **5**, 3096–3104.

43 N. Ferré and M. Olivucci, *J. Am. Chem. Soc.*, 2003, **125**, 6868–6869.

44 E. N. Laricheva, S. Gozem, S. Rinaldi, F. Melaccio, A. Valentini and M. Olivucci, *J. Chem. Theory Comput.*, 2012, **8**, 2559–2563.

45 T. Andruniów, N. Ferré and M. Olivucci, *Proc. Natl. Acad. Sci. U. S. A.*, 2004, **101**, 17908–17913.

46 S. Sekharan, M. Sugihara and V. Buss, *Angew. Chem., Int. Ed.*, 2007, **46**, 269–271.

47 S. Sekharan, M. Sugihara, O. Weingart, T. Okada and V. Buss, *J. Am. Chem. Soc.*, 2007, **129**, 1052–1054.

48 S. Sekharan, *Photochem. Photobiol.*, 2009, **85**, 517–520.

49 S. Gozem, M. Huntress, I. Schapiro, R. Lindh, A. A. Granovsky, C. Angeli and M. Olivucci, *J. Chem. Theory Comput.*, 2012, **8**, 4069–4080.

50 S. Gozem, F. Melaccio, R. Lindh, A. I. Krylov, A. A. Granovsky, C. Angeli and M. Olivucci, *J. Chem. Theory Comput.*, 2013, **9**, 4495–4506.

51 E. Walczak and T. Andruniów, *Phys. Chem. Chem. Phys.*, 2015, **17**, 17169–17181.

52 P. J. v. d. Tempel and H. O. Huisman, *Tetrahedron*, 1966, **22**, 293–299.

53 R. N. Gedye, P. C. Arora and K. Deck, *Can. J. Chem.*, 1971, **49**, 1764–1766.

54 J. W. Lewis, I. Pinkas, M. Sheves, M. Ottolenghi and D. S. Kliger, *J. Am. Chem. Soc.*, 1995, **117**, 918–923.

55 M. Groesbeek, R. van der Steen, J. C. van Vliet, L. B. J. Vertegaal and J. Lugtenburg, *Recl. Trav. Chim. Pays-Bas*, 1989, **108**, 427–436.

56 F. J. H. M. Jansen, M. Kwestro, D. Schmitt and J. Lugtenburg, *Recl. Trav. Chim. Pays-Bas*, 1994, **113**, 552–562.

57 W. Gaertner, P. Towner, H. Hopf and D. Oesterhelt, *Biochemistry*, 1983, **22**, 2637–2644.

58 E. Tajkhorshid, B. Paizs and S. Suhai, *J. Phys. Chem. B*, 1999, **103**, 4518–4527.

59 B. Honig, U. Dinur, K. Nakanishi, V. Balogh-Nair, M. A. Gawinowicz, M. Arnaboldi and M. G. Motto, *J. Am. Chem. Soc.*, 1979, **101**, 7084–7086.

60 M. Schreiber, M. R. Silva-Junior, S. P. A. Sauer and W. Thiel, *J. Chem. Phys.*, 2008, **128**, 134110.

61 M. Sugihara and V. Buss, *Biochemistry*, 2008, **47**, 13733–13735.

62 G. G. Kochendoerfer, P. J. E. Verdegem, I. van der Hoef, J. Lugtenburg and R. A. Mathies, *Biochemistry*, 1996, **35**, 16230–16240.

63 H. J. A. Dartnall, *Vision Res.*, 1968, **8**, 339–358.

64 M. Heck, S. A. Schadel, D. Maretzki, F. J. Bartl, E. Ritter, K. Palczewski and K. P. Hofmann, *J. Biol. Chem.*, 2002, **278**, 3162–3169.

65 R. Vogel, F. Siebert, G. Mathias, P. Tavan, G. Fan and M. Sheves, *Biochemistry*, 2003, **42**, 9863–9874.

66 B. Knierim, K. P. Hofmann, O. P. Ernst and W. L. Hubbell, *Proc. Natl. Acad. Sci. U. S. A.*, 2007, **104**, 20290–20295.

67 E. Hessel, M. Heck, P. Muller, A. Herrmann and K. P. Hofmann, *J. Biol. Chem.*, 2003, **278**, 22853–22860.

68 S. Jäger, K. Palczewski and K. P. Hofmann, *Biochemistry*, 1996, **35**, 2901–2908.

69 P. B. S. Dawadi and J. Lugtenburg, *Molecules*, 2010, **15**, 1825–1872.

70 W. Gärtner and S. Ternieden, *J. Photochem. Photobiol., B*, 1996, **33**, 83–86.

71 Q. Tan, K. Nakanishi and R. K. Crouch, *J. Am. Chem. Soc.*, 1998, **120**, 12357–12358.

72 M. E. Estevez, A. V. Kolesnikov, P. Ala-Laurila, R. K. Crouch, V. I. Govardovskii and M. C. Cornwall, *J. Gen. Physiol.*, 2009, **134**, 137–150.

73 M. Han, S. W. Lin, S. O. Smith and T. P. Sakmar, *J. Biol. Chem.*, 1996, **271**, 32330–32336.

74 M. Han, M. Groesbeek, T. P. Sakmar and S. O. Smith, *Proc. Natl. Acad. Sci. U. S. A.*, 1997, **94**, 13442–13447.

75 R. Nelson, J. K. deRiel and A. Kropf, *Proc. Natl. Acad. Sci. U. S. A.*, 1970, **66**, 531–538.